



Analysis of water chemical characteristics and application around large opencast coal mines in grassland: a case study of the North Power Shengli coal mine

Suping Peng^a, Feisheng Feng^{a,b,*}, Wenfeng Du^{a,b}, Yunlan He^{a,b}, Shan Chong^{a,b},
Zhenguo Xing^{a,b}

^aState Key Laboratory of Coal Resource and Safe Mining, China University of Mining & Technology, Beijing 100083, China, email: psp@cumtb.edu.cn (S. Peng), Tel. +86 188 1176 7893, email: tbp1600201014@student.cumtb.edu.cn (F. Feng), duwf66@126.com (W. Du), yunlanhe@pku.edu.cn (Y. He),

^bCollege of Geoscience and Surveying Engineering, China University of Mining & Technology, Beijing 100083, China, email: 396185870@qq.com (S. Chong), TSP1600201046@student.cumtb.edu.cn (Z. Xing)

Received 25 February 2018; Accepted 7 November 2018

ABSTRACT

Groundwater is the main source of water in the grassland in eastern China, this region is one of the largest coal bases in China. It is of great significance to study the influence of opencast coal mine exploitation on the chemical characteristics of groundwater in grassland and thus to evaluate the suitability of irrigation water based on changes in the chemical characteristics of water. To study the background values of the chemical characteristics of groundwater and thus to assess the effects of high-intensity coal mine exploitation on groundwater, the water samples in this study were obtained from the mining site, as well as from private wells and rivers. It is found that the dominant hydro-chemical types of the local surface water and groundwater are the $\text{Ca}^{2+}\text{-Mg}^{2+}\text{-HCO}_3^-$ and $\text{Na}^+\text{-Cl}$ types. The concentrations of Na^+ , HCO_3^- and SO_4^{2-} are relatively high in these water samples, and nearly all of them exceed those in the WHO and GB 5749-2006 standards. Both the shallow aquifer water and surface water samples exhibit high salinity, low and moderate alkalinity, and low conductivity, which indicates that they can be used for irrigation. However, the quality of the deep groundwater samples is Permissible to Doubtful, and the coal seam aquifer water is not suitable for irrigation due to its high salinity, high alkalinity and high conductivity. To guarantee the safe usage of domestic and irrigation water, mine drainage is an important alternative to alleviate the local water usage contradiction. The post-processing drainage of coal seam aquifers should be fully taken into consideration. A groundwater monitoring network around the mining area, including urban areas, should be established and improved. The coal seam aquifer water source should be adequately avoided during future well drilling.

Keywords: Mine water; High-intensity mining; Irrigation grades; Chemical characteristics

1 Introduction

It is estimated that 38% of global irrigation areas use groundwater as a water source [1]. As shown in Fig. 1, groundwater accounts for 98.55% of the irrigation water used for grassland, farmland and orchard in Xilinhot City, which is located in the grassland of eastern China [2]. Irriga-

tion water accounts for 51.95% of the city's total water consumption, as shown in Table 1. The exploitation of opencast coal mines will have an effect on the groundwater reserve and hydro-chemical characteristics of the grassland area, while the chemical parameters of groundwater will affect its suitability as irrigation water. Therefore, it is necessary to study the hydro-chemical characteristics of the groundwater around the opencast coal mine and to assess its suitability for use as irrigation water. The grassland in

*Corresponding author.

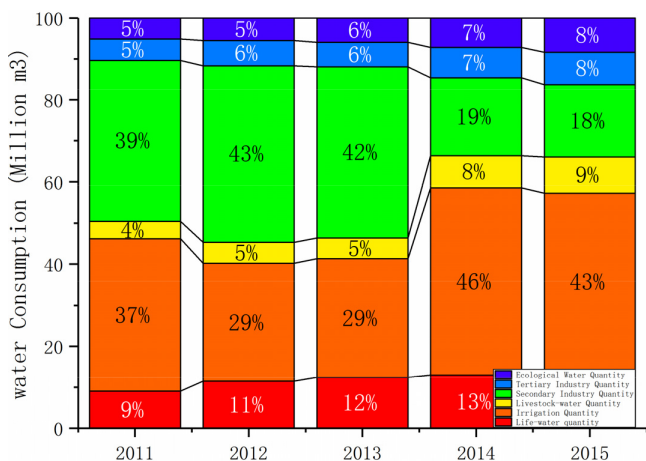


Fig. 1. The water consumption of various industries in Xilinhot City over the past five years.

eastern Inner Mongolia is a water-deficient and ecologically vulnerable area that relies heavily on groundwater. The annual output in the Shengli No. 1 coal mine, which is located in this region, can reach up to 16 million tons, where most of the coal seams have Quaternary aquifers with a thickness of 18–40 m [3,4]. Therefore, this paper evaluates the hydro-chemical characteristics of groundwater and the suitability of irrigation in the surrounding area of the large opencast coal mine by using the surrounding area of the Shengli No. 1 opencast coal mine as the study area. It is extremely challenging to create a large opencast coal mine in a grassland region exhibiting such a water shortage and strong groundwater dependence. The Shengli No. 1 opencast coal mine has an annual output of 16 million tons, and

most of its coal seams are suitable for opencast mining, even with an 18- to 40-m-thick Quaternary aquifer. Therefore, the analysis of the high-intensity exploitation of opencast coal mines can play a very important role in characterizing the chemical effects, classifying the irrigation grades and evaluating the groundwater in grassland pastoral areas.

After the 1970s, water-rock equilibrium began to be researched based on the principles of mass conservation, Gibbs free energy and the Nernst equation, and the quantitative analysis and prediction of the geochemical characteristics of groundwater were also initiated [5,6]. In recent years, researchers around the world have used different methods to analyze the chemical characteristics of the surface water and groundwater in various basins. Bhuiyan et al. used a comprehensive method based on the combination of the pollution evaluation index, principal component analysis and cluster analysis to evaluate the pollution levels and sources of irrigation water and drinking water in Bangladesh. The results showed that the water temperature, BOD, COD, Mn, Fe, Co, Ni, Cu and Pb contents in most water samples were higher than those in Bangladeshi and international standards [7].

At present, many scholars have studied the hydro-chemical characteristics of groundwater. Marković et al. conducted a statistical analysis of the chemical data from Zagreb-area groundwater in Croatia. It was found that although the aquifers in the study area form a single hydrogeological unit, their hydrogeochemistry exhibits obvious zonation, and the quality of deep underground water is better than that of shallow water. They also concluded that the weathering of carbonate and silicate rock plays an important role in the chemical composition of groundwater [8]. Shanyengana et al. discussed the groundwater salinization process in the Namib Desert and Northern Namibia using a graphic method. They found that the total dissolved

Table 1
Xilinhot 2011–2015 water consumption statistics table (unit: million m³)

Age	Life-water quantity				Primary industry quantity					
	Towns	Rural	Total	Including ground water	Agricultural irrigation	Forest and fruits	Grassland	Livestock	Total	Including ground water
2011	708	124	832	832	2765	654	0	392	3811	3811
2012	701	206	907	907	1759	514	0	407	2680	2680
2013	865	95	960	960	1683	550	0	390	2623	2623
2014	878	51	929	929	117	504	2646	557	3824	3824
2015	880	57	937	937	84	450	2336	583	3453	3403
Age	Secondary industry quantity				Tertiary industry quantity		Ecological water quantity		Total water consumption	
	Industry	Building	Total	Including ground water	Total	Including ground water	Total	Including ground water	Sum total	Including ground water
2011	3256	352	3608	3478	483	483	472	212	9206	8816
2012	3042	382	3406	3277	487	487	435	214	7915	7565
2013	2860	370	3230	3080	460	460	460	110	7733	7233
2014	1302	60	1362	1212	532	532	515	315	7162	6812
2015	1162	15	1177	1000	525	525	555	265	6647	6130

solid contents in groundwater vary greatly, and these contents can reach up to 500% in deep water areas or in areas in which underground water has been overexploited. It was proposed that the effects of evaporation, the dissolution of evaporated rock and mixing with salt water are the main hydrogeochemical processes that lead to salinization [9]. Vanderzalm et al. studied the main recharge sources of groundwater in the central Australia shallow alluvial plain and its hydrogeochemical evolution process by using a graphic method and ternary mixture model [10]. The results showed that the shallow groundwater in the alluvial plain mainly comes from river infiltration in flood periods, adjacent basin lateral recharge and deep groundwater leakage recharge in different sections. Cloutier et al. also studied the hydrogeochemical evolution of groundwater and obtained a more comprehensive understanding of the evolution of the groundwater dynamic field and chemical field by combining multivariate statistical methods. Based on the analysis of groundwater hydro-chemical parameters, some scholars have also evaluated the irrigation suitability of groundwater, especially in water-deficient areas [11]. Neves et al. evaluated the groundwater quality and environmental impact of abandoned uranium mines in central Portugal from 1995 to 2004. It was found that the concentrations of SO_4^{2-} , Al^- and Mn^{2+} were more than 50–120 times greater than those in the standard, resulting in the risk of soil degradation [12].

Singh et al. studied the major ion chemical characteristics and geochemical processes dominating the water composition of the surface water, groundwater and mine water in the upstream watershed of the Damodar River Basin in India and also evaluated the applicability of various kinds of water with different salinity, sodium, magnesium and SAR values to domestic, industrial and irrigation purposes [13,14]. Singh et al. also surveyed the hydrogeochemistry of coal mine drainage and evaluated the geochemistry and solute capture processes of mine water as well as its applicability to domestic, irrigation and industrial uses. Neogi et al. analyzed the water samples collected from various locations in the Karanpura coalfield mine, including their electrical conductivity values, total dissolved solids, total hardness, main anions, cations and trace metal ions, and evaluated the geochemical characteristics, acquisition processes, and dissolution flux of the mine water [15]. Tiwari et al. collected 30 different samples in the Bokaro coalfield and these samples were qualitatively assessed in terms of the domestic and irrigation applications of water in the Bokaro coal mine [16].

However, no research has investigated the chemical characteristics of groundwater and assessed its irrigation suitability in the vicinity of an opencast coal mine. Because of its location and production [17], the Shengli No. 1 opencast coal mine is an ideal location for this study [18,19]. First, it is located in the vicinity of the Xilin River and the hydro-chemical characteristics of the area surrounding the coal mine are closely related to the changes in the hydro-chemical characteristics in the downstream area. Second, all of the opencast stripped material of the Shengli No. 1 mine began to undergo internal dumping in 2012, and the internally dumped abandoned materials are mainly clay and shale, which can easily chemically react with water. For the purpose of mine safety, it is of great significance to maintain the stability of the inner dump and its slope.

Third, a pastoral area surrounds the mining area, and the local coal and animal husbandry industries are economic mainstays [20]. Therefore, it is very important to study the hydro-chemical characteristics of the groundwater in the areas surrounding the Shengli No. 1 opencast coal mine and evaluate its irrigation level for the development of the local economy. This study can also provide a reference for groundwater research in other mining areas under similar conditions.

2. Materials and methods

2.1. Study area description

The North Power Shengli No. 1 opencast coal mine (east longitude: $111^{\circ}16'37''$ – $111^{\circ}19'24''$, north latitude: $39^{\circ}50'04''$ – $39^{\circ}52'11''$) is one of the largest opencast mines in China. As shown in Fig. 2, its annual output reached 25 million tons in 2012 and 16 million tons in 2016. The main coal seams of the coal mine are the No. 5 and No. 6 coal seams, which have coal seam dip angles of less than 5° . The average thickness of the No. 5 coal seam is 18.16 m and the average thickness of the No. 6 coal seam is approximately 36.64 m. Single bucket and truck mining technology has been adopted here.

Shengli coalfield is located in the middle of Xilingol Grassland, which has a semi-arid steppe climate with a large annual temperature range. The maximum recorded temperature is 38.3°C (July 25, 1955), and the minimum recorded temperature is -42.4°C (January 15, 1953). The annual average number of days with temperatures below -25°C is 40.15 d, the annual average precipitation is 293.45 mm (1957–2004), and the annual average evaporation is 1794.64 mm (1974–2004). The freezing period lasts from the beginning of October to the first third of December every year. As shown in Table 2, the maximum depth of frozen soil is 2.89 m (1969), and the average depth of frozen soil is 2.42 m. The southern mine area is located 5 km from downtown Xilinhot, while its eastern, northern and western areas are pastoral areas. The Xilin River flows through the area located 400 m from the eastern part of the mine area.

2.2. Hydrogeology

The Shengli No. 1 opencast mine is a hydrogeological unit of the Xilin hot Basin. The aquifers that influence the opencast mining area include Quaternary pore aquifer, Top conglomerate segment aquifer, No. 5 seam fracture confined aquifer and No. 6 seam fracture confined aquifer. In essence, stably aquifuge exist between the above mentioned four aquifers, and their lithologies are dominated by mud stone, sandy mud stone and fine siltstone. The recharge of quaternary pore aquifer in the Shengli No. 1 open-air area is predominantly composed of precipitation, as well as the lateral recharge of the Xilin River, snow and ice melt water, atmospheric condensate and groundwater runoff. The recharge of the top conglomerate segment aquifer, No. 5 seam fracture confined aquifer and No. 6 seam fracture confined aquifer is mainly supplied by the concealed aquifer causing the infiltration of meteoric water into outcrops and the infiltration of transfluence into the local weak parts of the aquiclude.

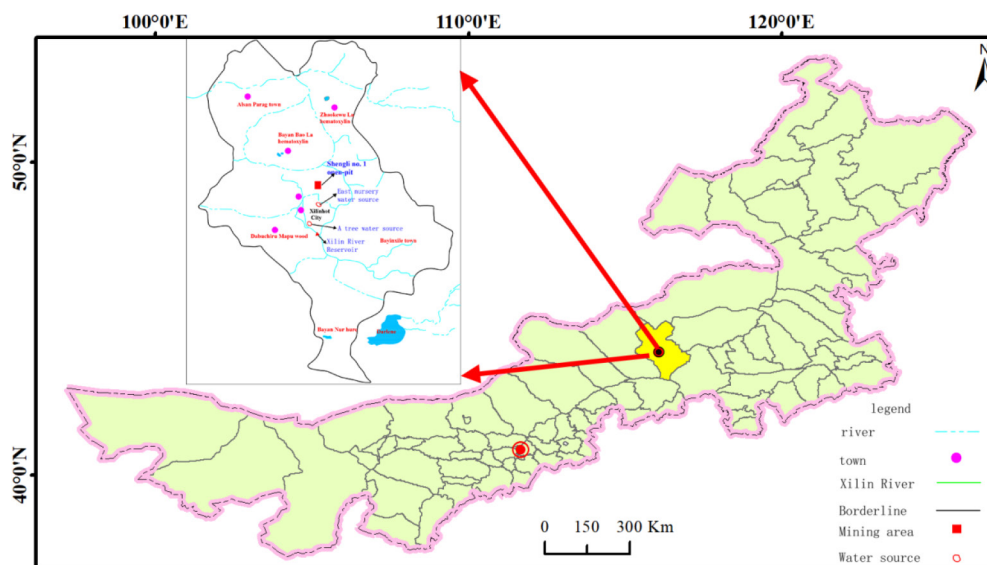


Fig. 2. Geographic location map of the North Power Shengli No. 1 opencast mine.

Table 2

Major weather indicators and output details of the Shengli No. 1 open pit mine in the last ten years

Age	Stripping/million m ³	Coal Yield/megaton	Rainfall	Evaporation	Temperature	Pumpage/million m ³
2007	38.50	6.19	150.5	1478.9	4.3	4.32
2008	50.86	10.85	228.6	1482	3.68	6.54
2009	59.33	10.53	240.8	1437.6	3.17	8.23
2010	33.56	14.25	276.9	1331.5	2.76	6.93
2011	78.31	24.42	226.7	1357.3	2.58	6.46
2012	93.65	24.91	511.7	1214.7	1.57	6.44
2013	37.36	17.89	273.4	1231	3.03	4.84
2014	46.02	17.02	255.9	1414.3	4.66	2.75
2015	35.34	12.08	412.8	1316.9	3.9	2.40
2016	45.58	16.00	309	1346.2	3.42	2.61

The Xilin River is the lowest erosional base in this area. The Xilin River valley alluvial plain is dominated by groundwater runoff and evaporation discharge. Sewer drainage of Quaternary aquifers and coal seam aquifers is another drainage method in the region. Three faults are developed in the first mining area of the Shengli No. 1 opencast area. F1, F25 and F29 are normal faults that are NE-trending, with dip angles of greater than 50°, which are mainly characterized by compresso-shear features. The fault zone is mainly composed of mud stone and plastic rock cemented with mud stone, with few cracks and an undeveloped fractured zone that can be considered an aquiclude. The Xilin hot reservoir, founded in 1958, is located 9 km to the south of Xilin hot City and currently has a total reservoir storage capacity of 19.0 Mm³. As shown in Fig. 3, its water level reaches up to 1011.87 m.

2.3. Groundwater sampling and ion analysis

Due to the reconstruction and extension of the mining area, most of the observation wells in the mining area were

damaged, and there is no systematic long-term dynamic observation network for the groundwater environment around the mining area.

By analyzing the Shengli No. 1 opencast coal mine data to assess the hydrogeological conditions and characteristics of the mining area, we found 9 representative sites. These sites represent all of the important change points and important applied fields related to the groundwater circulation in this region: SL#1, 3, 5, 6, 7, 9, 11, 13 and 15 are the sites corresponding to coal mine water, coal seam direct infiltration water, Xilin River reservoir water, the groundwater used for landscaping near the reservoir, the vegetable base groundwater 2 km from the southeastern region of the mining area, the cow village pressure well, the well of the No. 1 herdsman's family, the well of the No. 2 herdsman's family, and the water drained outwards after undergoing mine water treatment, respectively. The water depths of SL#6, 7, 9, 11, and 13 are 15 m, 9.2 m, 7.3 m, 93 m and 24 m, respectively. The water sampling points for SL#6, 7, 9, 11 and 13 are 16 m, 80 m, 8.3 m, 94 m and 25 m above the Earth's surface, respectively.

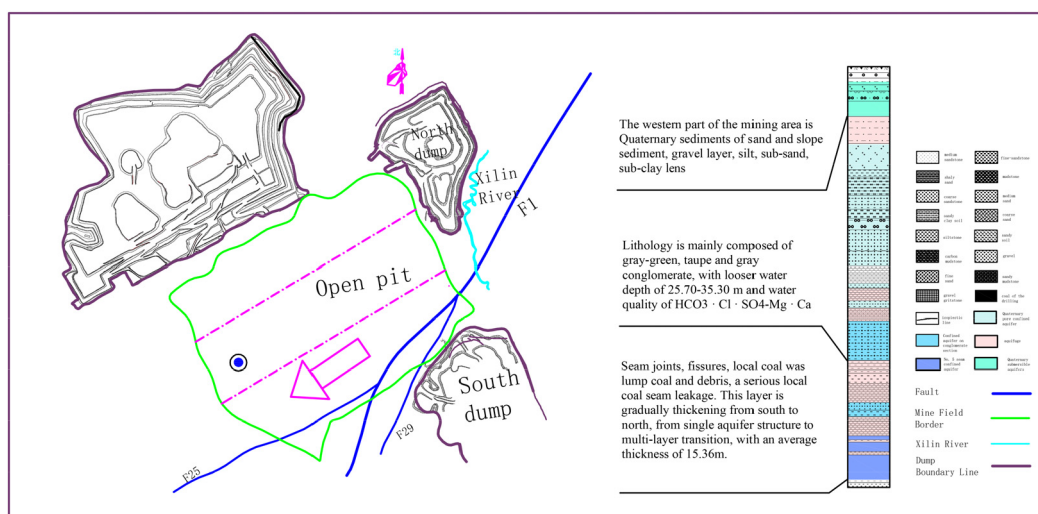


Fig. 3. Comprehensive schematic diagram of the hydrogeological structure in the mining area.

The groundwater sampler is a 1.5 L sampling bottle with a 2 kg steel column bottle hanging below it, and it contains ten holes with diameters of 1–2 mm that are located close to the mouth of the upper bottle. Before the water sampling process, the sampler cover cap is tightened. When the sampler comes in contact with the water surface in the drill, the rope is rapidly released as required every 1 m, 5 m or 10 m. After waiting 3–5 min, the bottle is quickly pulled to the ground and unscrewed, and the water is poured out quickly, thus avoiding prolonged contact with air and affecting the accuracy of the analysis.

3. Results

3.1. Anion and cation chemistry

The statistics of the water chemistry parameters are shown in Table 3. The majority of the water samples in the study area comprise HCO_3^- and SO_4^{2-} . The average concentrations of the four anions of HCO_3^- , SO_4^{2-} , Cl^- and NO_3^- are 541.57, 232.05, 141.33 and 18.73 mol/L, respectively. To accurately compare these samples, the contribution percentages of various ions are shown in Fig. 4.

The concentrations of HCO_3^- range from 332.3 mg/l (SL#13) to 674.20 mg/l (SL#15), and their ratios to the average value range from 0.61–1.24. The concentrations of SO_4^{2-} range from 37.28 mg/l (SL#5) to 535.55 mg/l (SL#1), and their ratios to the average value range from 0.16–2.31. The concentrations of Cl^- range from 58.08 mg/l (SL#13) to 192.25 mg/l (SL#15), and their ratios to the average value range from 0.41–1.36. Two samples with the lowest HCO_3^- concentration are SL#13 and SL#5. There is no evidence indicating that HCO_3^- can cause harm to the human body. According to the requirements of the WHO [21], safe and reasonable concentrations of HCO_3^- are less than 300 mol/L. The bicarbonate concentration in the groundwater mainly depends on the alkalinity. When carbon dioxide in the atmosphere and the soil dissolves into the groundwater, it forms bicarbonate.

The concentrations of SO_4^{2-} in these samples range from 37.28 to 535.55 mol/L. According to the Chinese

national standard [22], the SO_4^{2-} concentration of class III water should be less than 250 mol/L. Thus, samples SL#1, SL#3, SL#11 and SL#15 are not consistent with these drinking water standards. It is interesting to note that of these four water samples, three were obtained within the mining area exhibit relatively high concentrations in the range of 280.78–535.55 mol/L. However, the other sample is SL#11, whose concentration of SO_4^{2-} reaches an astonishing 405.57 mol/L. This concentration ranks only second to the seepage of the no. 5 coal in SL#1, which was obtained from the deep well of a herdsman's family located far from the mining area. Coal mining accelerates the strong oxidation of certain minerals (e.g., pyrite) in a rock, which influences its SO_4^{2-} concentration. More surveys [23,24] of the background concentration values in deep water sources are required to clarify the reasons for the high SO_4^{2-} concentration of SL#11 and to determine measures for its avoidance [25]. The changes in Cl^- concentrations are very similar to those in HCO_3^- , indicating that there was a strong correlation between them. Thus, this required the correlation analysis of the chemical ions in groundwater.

For these four kinds of cations, their concentrations rank at every sampling point is $\text{Na}^+ > \text{Ca}^{2+} > \text{Mg}^{2+} > \text{K}^+$, indicating that their ion concentration ratios are basically stable, and their average concentrations are 236, 73, 41 and 7 mol/L, respectively.

The concentrations of Na^+ range from 100.5 mg/l (SL#5) to 422 mg/l (SL#3), and their ratios to the average value range from 0.43–1.78. The concentrations of Ca^{2+} range from 29.43 mg/l (SL#3) to 115.29 mg/l (SL#9), and their ratios to the average value range from 0.40–1.57. The concentrations of Mg^{2+} range from 15.37 mg/l (SL#3) to 70.41 mg/l (SL#1), and their ratios to the average value range from 0.37–1.69. The concentrations of K^+ range from 1.38 mg/l (SL#13) to 15.16 mg/l (SL#5), and their ratios to the average value range from 0.17–1.90. It can be seen that the discrete distribution of each cation falls within a relatively stable interval, wherein Na^+ has the highest concentration in the groundwater of the study area and K^+ has the lowest concentration in the groundwater of the study area [26]. From a macro-scale perspective, the local high Ca^{2+} concentrations

Table 3
Water chemistry statistics table

Sample ID	K ⁺	Na ⁺	Ca ²⁺	Mg ²⁺	HCO ₃ ⁻	Cl ⁻	SO ₄ ²⁻	NO ₃ ⁻	TDS	NO ₂ ⁻
SL#1	8.44	326	95.66	70.41	587.7	175.42	535.55	5.13	1516.54	0.03
SL#3	6.32	422	29.43	15.37	669.5	184.68	280.78	0.12	1281.92	0.02
SL#5	15.16	100.5	41.7	35.2	419.6	77.53	37.28	2.37	523.99	0
SL#6	11.44	108	76.04	39.67	506	105.73	55.32	4.5	658.86	0.01
SL#7	4.82	278	82.58	34.71	611.3	155.83	228.94	47.05	1143.76	0
SL#9	11.36	128	115.29	45.62	589.5	160.25	58	1.79	821.34	0
SL#11	3.52	278	71.14	54.54	484	162.23	405.57	5.08	1227.15	0.01
SL#13	1.38	122.5	70.32	24.3	332.3	58.08	96.49	99.26	641.9	0.01
SL#15	9.2	364	78.49	53.55	674.2	192.25	390.53	3.23	1435.16	0

Sample ID	Total hardness	Salinity	Free CO ₂	H ₂ SiO ₃	Soluble SiO ₂	Conductivity	Total Iron	Ammonia Nitrogen	Nitrate nitrogen	Nitrite Nitrogen
SL#1	529.31	1804.51	34.73	15.5	11.92	2390	0.26	0.14	1.16	0.009
SL#3	136.89	1609.97	10.22	15.08	11.6	2190	0.33	1.37	0.03	0.006
SL#5	249.33	729.59	32.69	17.38	13.37	945	0.18	0.19	0.53	0.001
SL#6	353.53	906.8	20.43	24.44	18.8	1197	0.05	0.07	1.02	0.002
SL#7	349.4	1443.29	44.95	22.66	17.43	1878	0.3	0.05	10.62	0.001
SL#9	476.09	1110.2	42.98	30.19	23.22	1484	0.18	0.3	0.4	0.001
SL#11	402.61	1464.31	10.22	15.16	11.66	2020	0.07	0.18	1.15	0.002
SL#13	275.85	804.72	12.26	16.77	12.9	1091	0.08	0.07	22.41	0.002
SL#15	416.89	1765.52	24.52	24.08	18.52	2390	0.05	0.05	0.73	0.001

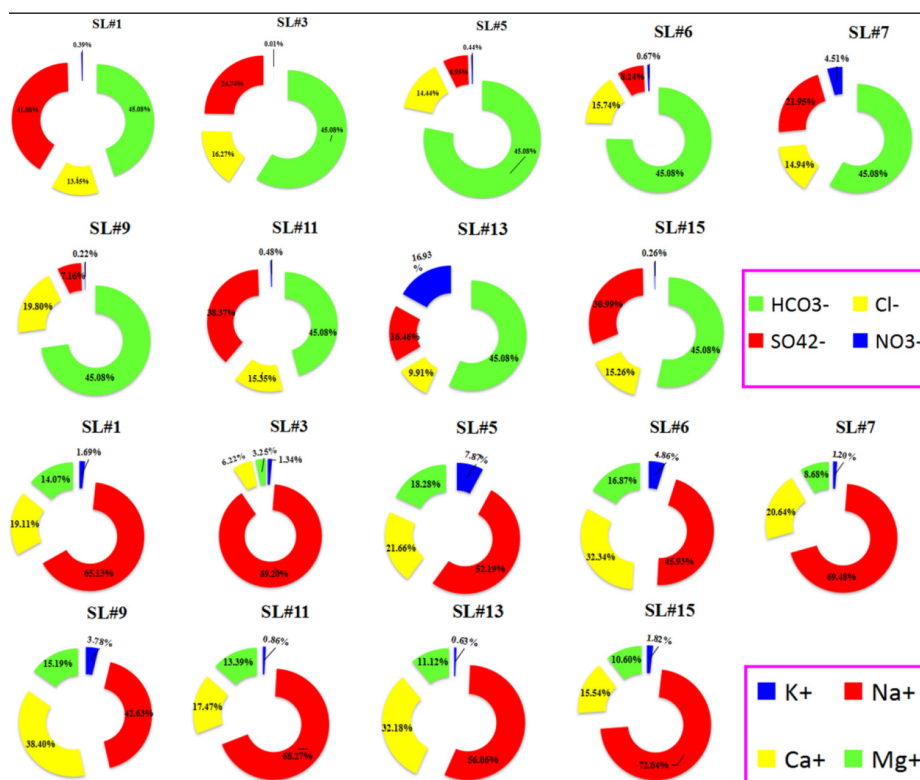


Fig. 4. Pie chart of the concentration ratios of anions and cations.

may due to the fact that most rocks contain minerals and all water-bearing units may be influenced by water-rock interactions. The reason for the lowest K^+ concentration may be that K^+ can be easily consolidated by clay minerals. This change in ion concentrations is particularly evident at the regional scale [27,28], suggesting that there are many clay minerals in the study area.

According to the Shoka Lev classification method, SL#3 and SL#7 are 7-B, SL#5 is 7-A, SL#1 and SL#15 are 14-B, SL#11 is 14-A, and SL#6, SL#9, and SL#13 are 4-A type water.

3.2. Spatial distribution characteristics of water quality components

The spatial distribution of water quality constituents is shown in Fig. 5. This figure shows that the distributions of conductivity, salinity and total dissolved solids (TDS) are highly consistent, with values ranging from 1091–1307 mg/L, 803–1804 mg/L, and 641–1511 mg/L, respectively. In general, TDS significantly exceeded the limit in the mining area but remained at relatively low levels in the northern pastoral area and the eastern village. The total hardness levels in the mining area are low in the northern pastoral area and high in the eastern village, which is mainly due to the high Ca^{2+} content of the SL#9 water sample [29–31].

4 Discussion

4.1. Analysis of groundwater chemical correlation

Correlation analysis can reveal the similarities and differences between the chemical parameters of groundwater and the similarities and differences in their sources. The intensity of the correlation is expressed by the Pearson correlation coefficient. The results of the Pearson correlation analysis are shown in Table 4.

The calculation results show that the correlation coefficients of Na^+ , SO_4^{2-} and Cl^- in the groundwater samples in the study area are very high. Their total regression equations are as follows:

$$Y = 2.7747x_1 + 372.1, r = 0.92196 \quad (1)$$

$$Y = 1.9102x_2 + 584.59, r = 0.94034 \quad (2)$$

$$Y = 6.7573x_3 + 72.808, r = 0.8843 \quad (3)$$

wherein y , x_1 , x_2 and x_3 (in mol/L) are the total mass concentration of dissolved solids, the sodium ion mass concentration, the sulfate ion mass concentration and the chlorine mass concentration, respectively. In addition, all of the Pearson coefficients between Na^+ and HCO_3^- , Cl^- , SO_4^{2-} , and TDS are greater than 0.8, further showing that sodium is the dominant cation. The Pearson coefficients between Mg^{2+} and Ca^{2+} and SO_4^{2-} are slightly larger than 0.6, indicating they exhibit a certain correlation. There is a significant correlation between HCO_3^- and Cl^- , whose Pearson coefficient reaches 0.91495. In addition, these data demonstrate that NO_3^- has a negative correlation with almost all other parameters. Considering that SL#5 is surface reservoir water, while SL#6 represents the shallow groundwater near the reservoir. These data indicate that their water quality has not been affected by any production activities, which is also why we chose these two samples to represent the background values of the regional surface water. The Na^+ concentrations of samples 7 and 11 vary between 250–300 mol/L, mainly because these are deep groundwater samples with relatively high concentrations.

The ratio between ions is an important factor used to indicate the chemical characteristics of groundwater. $\gamma Na^+ / \gamma Cl^-$ is known as the genetic coefficient of groundwater, which is a hydrogeochemical parameter used for characterizing the concentration of sodium ions in groundwater.

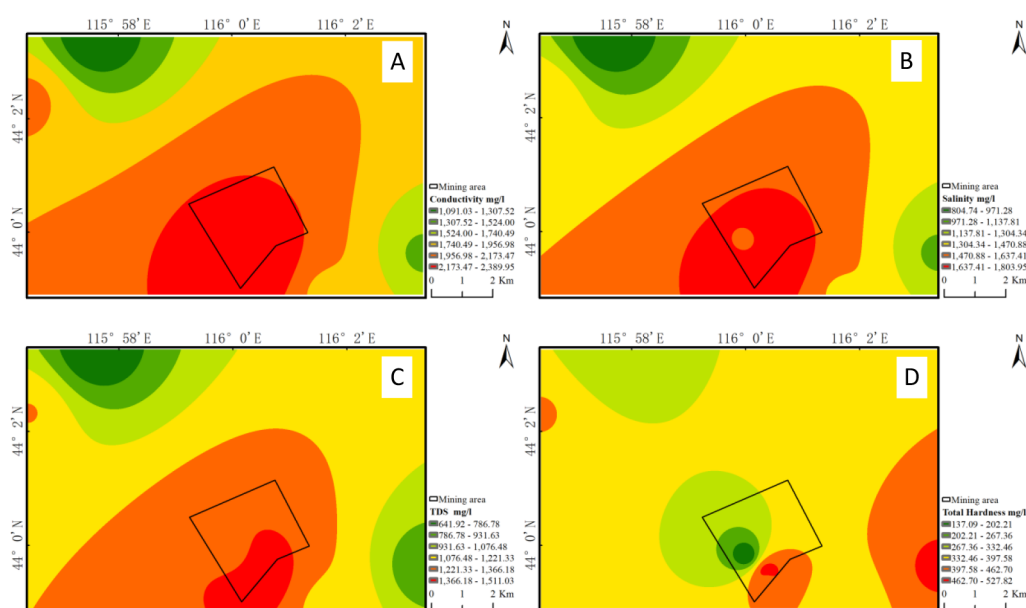


Fig. 5. Spatial distribution maps of different water quality constituents: conductivity (A), salinity (B), TDS (C) and total hardness (D).

Table 4
Pearson correlation analysis results

K ⁺	Na ⁺	Ca ²⁺	Mg ²⁺	HCO ₃ ⁻	Cl ⁻	SO ₄ ²⁻	NO ₃ ⁻	TDS	NO ₂ ⁻	Total Iron
1	-0.33892	0.01548	0.18912	0.13669	-0.05944	-0.34646	-0.66357	-0.30795	-0.25449	-0.01336
	1	-0.21401	0.12974	0.74682	0.82784	0.81407	-0.28152	0.92196	0.42254	0.43007
		1	0.6328	0.13746	0.21688	0.1016	0.03625	0.12956	-0.10992	-0.18259
			1	0.19411	0.40257	0.60754	-0.39894	0.47997	0.20284	-0.23465
				1	0.91495	0.48054	-0.56411	0.73238	0.09442	0.45011
					1	0.71451	-0.56786	0.8843	0.22196	0.34928
						1	-0.24888	0.94034	0.56361	0.17363
							1	-0.3131	-0.08956	-0.10689
								1	0.45283	0.31318
									1	0.32924
										1

Low-salinity water has a relatively high $\gamma\text{Na}^+/\gamma\text{Cl}^-$ coefficient ($\gamma\text{Na}^+/\gamma\text{Cl}^- > 0.85$), while high-salinity water has a relatively low $\gamma\text{Na}^+/\gamma\text{Cl}^-$ coefficient ($\gamma\text{Na}^+/\gamma\text{Cl}^- < 0.85$) [32]. In addition, the values of $\gamma\text{SO}_4^{2-}/\gamma\text{HCO}_3^-$, $\gamma\text{Cl}^-/\gamma\text{HCO}_3^-$, $\gamma\text{SO}_4^{2-}/\gamma\text{Cl}^-$, $\gamma\text{Mg}^{2+}/\gamma\text{Ca}^{2+}$ and $\gamma\text{Na}^+/\gamma\text{Cl}^-$ are also listed in Table 5.

The value of $\gamma\text{SO}_4^{2-}/\gamma\text{HCO}_3^-$ is generally considered to be an important chemical indicator in determining the water source. If it is greater than 1, the water source mainly comes from gypsum or salt. If it is less than 1, the water source is much more influenced by carbonate. The values of $\gamma\text{SO}_4^{2-}/\gamma\text{HCO}_3^-$ for samples from the researched area are all less than 1, indicating that groundwater in this region is more affected by carbonate sources [33]. The values of $\gamma\text{Cl}^-/\gamma\text{HCO}_3^-$ and $\gamma\text{Mg}^{2+}/\gamma\text{Ca}^{2+}$ are in a relatively stable level, and their values for samples from other sites are greater than 1. The values of $\gamma\text{SO}_4^{2-}/\gamma\text{Cl}^-$ for SL#5, SL#6 and SL#9 are less than 1, indicating there are no rock strata with sulfate ions in these three sites. All these three rock strata are typical layer where surface water exists, therefore it is certain that there are minerals that can produce sulfate in the deep part of strata.

The values of $\gamma\text{Na}^+/\gamma\text{Cl}^-$ for 8 of the 9 groups of water samples from the researched area are greater than 1, indi-

cating that the Na^+ concentration is basically greater than the Cl^- concentration. Since the values of $\gamma\text{Na}^+/\gamma\text{Ca}^{2+}$ and $\gamma\text{Na}^+/\gamma\text{Mg}^{2+}$ are all greater than 1, it can be considered that Na^+ was continuously released from the feldspar as the rock minerals are weathered and dissolved by hydrolysis and acid in the groundwater runoff process.

As the North Power opencast mine is located in the Xilin hot basin hydrogeological unit, the gentle slope hills in the Xilin River west and valley alluvial plain transition zone, gentle slope hills in the west, valley alluvial plain in the east, junction area of gentle slope hills and valley alluvial plain in the central west. Surface topography of the opencast area appears to be high in the northwest and low in the southeast. Surface water flow direction is from the southeast to the northwest, so the velocity is slow. Especially when the water-bearing media contains more clay minerals (as shown in Fig. 3), and the adsorption effect is more obvious. Ca^{2+} and Mg^{2+} in groundwater are adsorbed and exchanged releasing Na^+ into the underground water. Moreover, annual evaporation in Xilinqol pastoral area is far greater than the rainfall and the surface salinization phenomenon is very serious. Since a large number of fractures connected surface and under-

Table 5
The ion ratios in different samples

Sample ID	$\gamma\text{SO}_4^{2-}/\gamma\text{HCO}_3^-$	$\gamma\text{Cl}^-/\gamma\text{HCO}_3^-$	$\gamma\text{SO}_4^{2-}/\gamma\text{Cl}^-$	$\gamma\text{Mg}^{2+}/\gamma\text{Ca}^{2+}$	$\gamma\text{Na}^+/\gamma\text{Cl}^-$	$\gamma\text{Na}^+/\gamma\text{Ca}^{2+}$	$\gamma\text{Na}^+/\gamma\text{Mg}^{2+}$
SL#1	0.91	0.30	3.05	0.74	1.86	3.41	4.63
SL#3	0.42	0.28	1.52	0.52	2.29	14.34	27.46
SL#5	0.09	0.18	0.48	0.84	1.30	2.41	2.86
SL#6	0.11	0.21	0.52	0.52	1.02	1.42	2.72
SL#7	0.37	0.25	1.47	0.42	1.78	3.37	8.01
SL#9	0.10	0.27	0.36	0.40	0.80	1.11	2.81
SL#11	0.84	0.34	2.50	0.77	1.71	3.91	5.10
SL#13	0.29	0.17	1.66	0.35	2.11	1.74	5.04
SL#15	0.58	0.29	2.03	0.68	1.89	4.64	6.80

ground space are formed, it will bring the sodium ion into the groundwater when it rains, which is one of the reasons why Na^+ concentration is high in the vicinity of coal mine [34].

Fig. 6 illustrates that the discrete distribution effect of the data is excellent. We can accurately see that most of the data fall within a normal range, but a few abnormal data points appear in the Ca^{2+} and NO_3^- plots. Ca^{2+} content is abnormally high in SL#9, reaching up to 115.29 mol/L, and abnormally low in SL#3 and SL#5, reaching values of 29.41 and 41.7 mol/L, respectively, with a mean Ca^{2+} concentration of 73.41. Compared to the background values of countries such as India [35,36], United States [37,38], Iran [39,40] and regions of Xilinhot, which is located near the study area [41,42], the Ca^{2+} concentration in the study area is relatively high (41.7 mol/L), implying that the overall local Ca^{2+} concentration is high. The NO_3^- concentration of SL#7 is 47.05 mol/L, and the concentration of SL#13 is 99.26 mol/L, while the mean value is 18.73 mol/L. The ammonia nitrogen concentration of SL#3 is 1.37 mol/L, while the mean value is 0.27 mol/L.

Fig. 7 is the graphical representation of the main anions and cations in the water samples. These data are widely used to evaluate the relationship between the dissolved ionic components and the main water types [43]. The geochemical data on the trilinear diagram show that all points in the cation triangle are distributed in the Na^+ type region and the non-dominant ion area, while all points in the anion triangle are distributed in the HCO_3^- type region and the non-dominant ion area. The data diagram in the center of the diamond field also shows an interesting phenomenon in which almost all chemical types of the water samples can be classified into two categories, namely, the $\text{Ca}^{2+}\text{-Mg}^{2+}\text{-HCO}_3^-$ type and the $\text{Na}^+\text{-Cl}^-$ type. There are no coincident properties between these two chemical types. Therefore, these water samples either originated from different sources or were derived from the same source but experienced significant changes in their original chemical properties due to external effects.

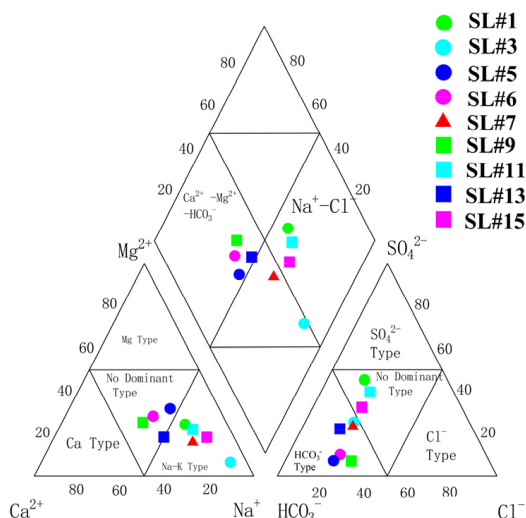


Fig. 7. Piper trilinear diagram analysis results.

Therefore, it is necessary to determine the specific reasons for changes in water quality, combined with the specific sources of water sampling points, the geological conditions at sampling points, and the relationship between sampling points and the mining area, etc. The Radar chart can connect all of the important elements in groundwater together, and users of this chart can directly observe the concentrations of various ions and the proportional relationships between them. When combined with Google Earth, this tool can be used to clearly and quickly observe changes in the content of water quality as well as the geographical reasons for these changes, as shown in Fig. 8.

It can be clearly seen that the ion content distributions of 5 and 6 are quite similar, followed by 9 and 13, which merely differ from 5 and 6 in terms of their HCO_3^- contents. The contents of samples 11, 1, 15, 3 and 7 are similar. From a geographical perspective, it can be seen that

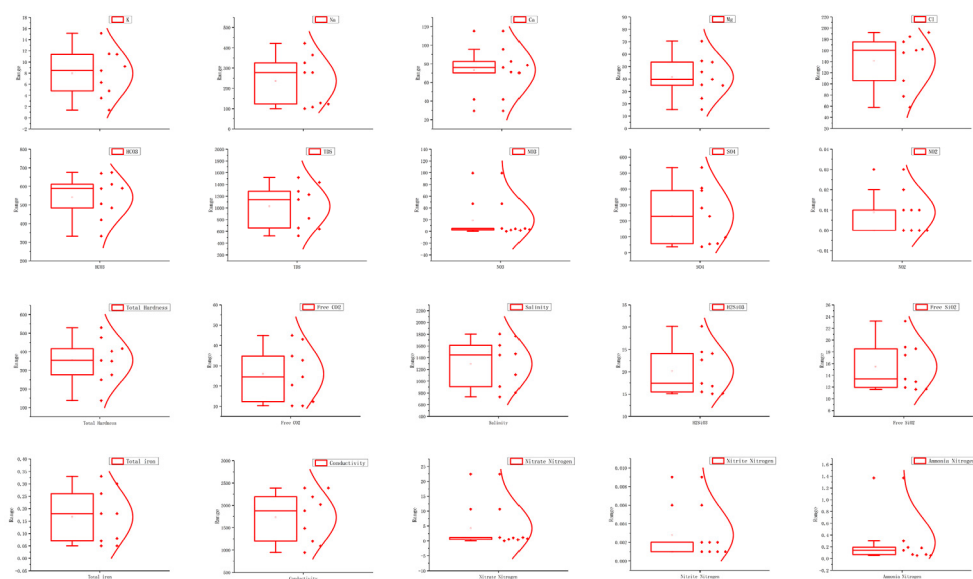


Fig. 6. Box plot analysis.

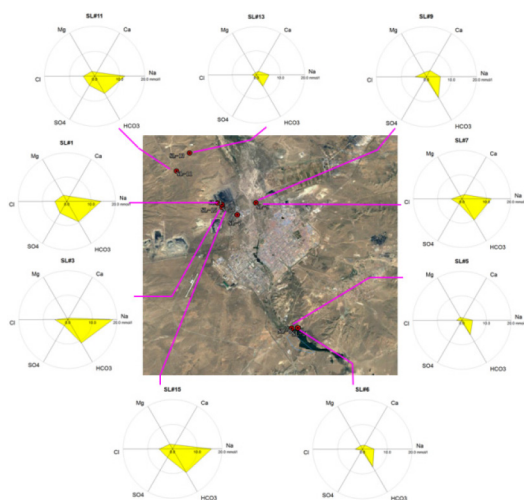


Fig. 8. Analysis results of Radar chart.

samples 5 and 6 are located 17 km away from the mine and located in the upstream region. As previously mentioned, these two points can be used as samples of surface water and unconfined water, respectively. Samples 9 and 13 are similar. Sample 9 is located in the cow village 3 km to the east of the mining area, and 13 is located in the pastoral area in the mining area 7 km to the northwest of the mining area. These four points are far from each other and separated by the mining area in the center. The reason for their similar ion contents and distributions is that they all comprise shallow groundwater. To some extent, these four samples also represent the background values of the hydro-chemical characteristics in this local region. Samples 11, 1, 15, 3 and 7 are similar, wherein 1, 3 and 15 are inner mine water samples. Analyzing them based on their water flow sequence reveals that the mine seepage water 3 outflows from the seepage point and through the mine bottom side slope, it then converges to the underground water collecting pit, which is water sampling point 1. After undergoing a simple treatment in the water collecting pit, the water is discharged and comes to sampling point 15. The above three points thus share a certain and unique source. The drilling data of the ten geological boreholes BK71-BK81 (as shown in Fig. 3) reveal that the distance between the no. 5 coal seam (aquifer) and the Earth's surface ranges from 50–65 m. Thus, the similarity between 11 and 7 indicates that they are water from the same aquifer or underground water from the same aquifer. Therefore, all 9 sampling points in this paper can be classified as four categories. Sample 5 is surface water, whereas 6, 9 and 13 are shallow groundwater, 7 and 11 are deep groundwater, and 3, 1 and 15 are inner water of the mining area.

The cluster analysis method is used to analyze all of the elements, as shown in Fig. 9.

If all of the samples are divided into 2 categories, the first category comprises samples 1, 15, 7, 11 and 3, while the second category comprises samples 5, 13, 6 and 9. The former category can be classified as deep groundwater, the latter category can be classified as surface water and shallow groundwater with similar chemical properties.

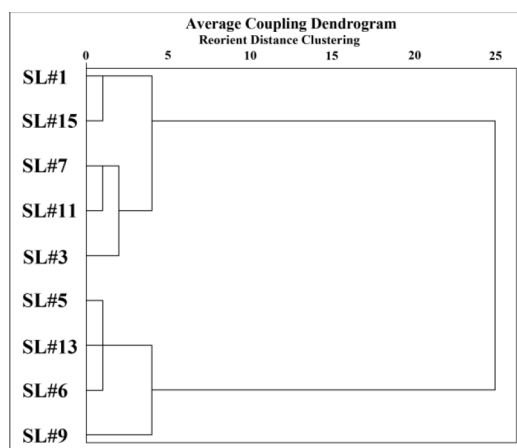


Fig. 9. Cluster analysis results.

If all of the samples are divided into 4 categories, the first category comprises samples 1 and 15, in which their only difference is that sample 15 represents sample 1 after undergoing a simple precipitation treatment. The second category comprises samples 7, 11 and 3, which can be identified as deep groundwater. The third category comprises samples 5, 13 and 6, which represent shallow groundwater or surface water. The fourth category comprises samples 9, on whose surface floating oil was recognizable during sampling, indicating that its water quality is not good due to man-made pollution and that it thus can be characterized as unusual shallow water.

If one subdivides these samples again, it can be found that samples 7, 11 and 3 can be divided into two classes, wherein sample 3 is water in the no. 5 coal seam aquifer, while samples 7 and 11 are mixed groundwater containing water from the no. 5 coal seam aquifer and other aquifers.

The above analysis demonstrates that the chemical characteristics of all samples are similar but gradually change. As the Piper trilinear diagram of all points is relatively concentrated and continuous, this process of change is continuous. However, all the regions formed together by all of the points nearly gradually change across two types of different regions. Through mathematical and statistical analysis, we can also find that the major reason for the changes in the chemical characteristics of the water samples due to their different sources of aquifers.

4.2. Evaluation of irrigation suitability

The Shengli coal mine is surrounded by pastoral areas, as it is located in the world-renowned prairie of the Xilingol Grassland. Since it was mentioned above that the water in the study area is not suitable for drinking, it is worth discussing if this water is suitable for agricultural irrigation. The Na and SAR contents in groundwater samples can affect the replacement of cations in clay minerals, resulting in increased sodium or causing damage to the permeability of the soil [44,45]. EC values can be used to reflect the TDS concentrations in groundwater [46]. Therefore, using the Na⁺, SAR and EC values as a classification standard, the Wilcox diagram [47] and the famous US Salinity Laboratory classification diagram were used to evaluate the

level of irrigation water [48]. The Wilcox diagram considers the percentages of both Na and EC, and it divides samples into five categories, namely, C1S1, C2S1, C2S2, C3S1 and C4S1, which correspond to Excellent to Good, Permissible to Doubtful, Good to Permissible, Doubtful to Unsuitable, and Unsuitable, respectively. The calculation formulas for SAR are shown as formulas (4) and (5), and the calculation results are shown in Table 6.

$$SAR = \frac{Na^+}{\sqrt{\frac{(Ca^{2+} + Mg^{2+})}{2}}} \quad (4)$$

$$\%Na^+ = \frac{K^+ + Na^+}{K^+ + Na^+ + Ca^{2+} + Mg^{2+}} \times 100\% \quad (5)$$

where SAR is the sodium adsorption ratio (mmol·L⁻¹)^{1/2}, and (Ca²⁺, Mg²⁺, Na⁺, K⁺) are the ion concentrations (mmol·L⁻¹).

Fig. 10 shows that 4 of our samples clearly fall in the range of good to permissible, indicating that they can be used as irrigation water. These samples include sample No. 5 of the Xilin River Reservoir, sample 6 of the shallow groundwater near the reservoir, sample 9 from the cow village pressure well and sample 13 from the No. 1 Herdsman. The vegetable base sample is permissible to doubtful, while the remaining 4 samples are all doubtful to unsuitable, including sample 1 of the pit water collected from the mining area, sample 3 of the no. 5 coal seam infiltration water, sample 15, which represents the mine water sample obtained after undergoing a simple treatment, and sample 11 from the deep groundwater from the No. 2 Herdsman's family.

Fig. 11 shows that samples 5, 6, 9 and 13 have high salinity and low alkalinity, two samples have high salinity and moderate alkalinity, one sample has high salinity and extremely high alkalinity, and the other two samples have extremely high salinity and high alkalinity. Thus, the results of these two evaluation methods are basically consistent.

The above analysis shows that the shallow groundwater and surface water in the study area are good to permissible. The shallow groundwater around the mining area can be used for irrigation in pastoral areas. The coal pit water and no. 5 coal seam aquifer well water are currently not suitable for direct irrigation applications due to their high salinity and alkalinity. However, after undergoing appropriate treatment, they can be used for agricultural irrigation. Therefore, based on this situation, joint efforts from the government, coal mining staff and herdsman are required to ensure the safety of living and irrigation water, as well as the proper and clean mining of local coal resources. It is necessary to formulate plans

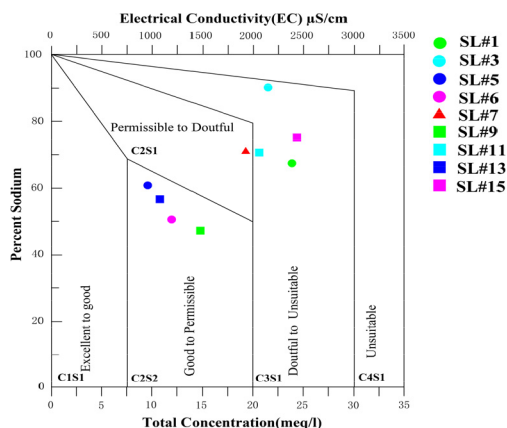


Fig. 10 Wilcox diagram.

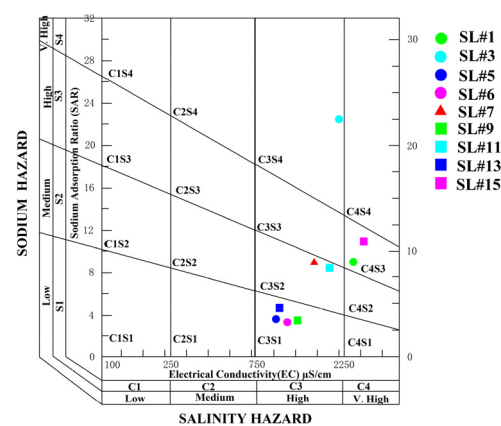


Fig. 11. Famous US Salinity Laboratory classification diagram.

and policies for water-saving irrigation, provide necessary financial support for water-saving projects, and establish and improve a groundwater monitoring network around the mining area. The layout of the drilling monitoring system is shown in Fig. 12. The monitoring system is principally based on a radial pattern of borehole distribution around the mining site. The boreholes outside the mining area are mainly used to maintain the water supply, with monitoring as a supplementary function, which improves efficiency and reduces the cost. The Quaternary pore aquifer is partly connected with the aquifer of the top conglomerate section, and they communicate with each other. In the eastern region of the mining area, a 5th coal outcrop was exposed and the aquifer of the upper conglomerate section is absent. Moreover, there are abundant hydrological boreholes in the quaternary system. Therefore, it is not necessary to arrange hydrogeological boreholes for verifi-

Table 6
Calculation results of Na⁺, SAR and EC

Sample ID	SL#1	SL#3	SL#5	SL#6	SL#7	SL#9	SL#11	SL#13	SL#5
SAR	8.69	22.12	3.9	3.52	9.12	3.6	8.49	4.53	10.93
EC	2390	2190	945	1197	1878	1484	2020	1091	2390
%Na ⁺	66.82	90.53	60.06	50.79	70.69	46.41	69.14	56.7	73.87

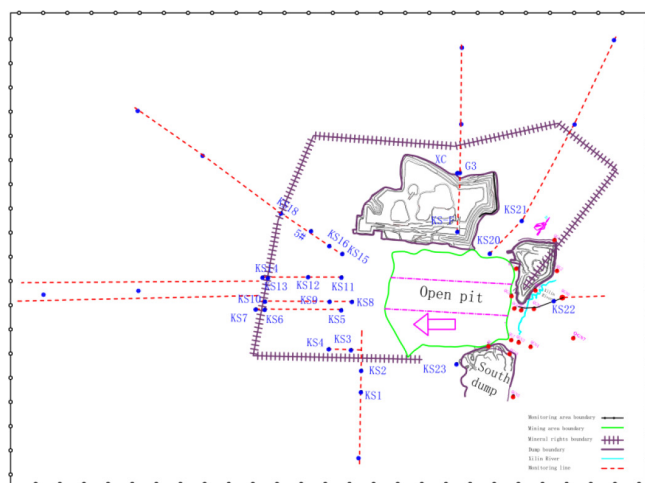


Fig. 12. Radial monitoring drilling layout.

cation. The exploration results show that the 5th coal seam group in the east has a relatively small range available for mining, so it is not necessary to arrange the observation section for the 5th coal seam group. In the dump along the roadside in the north, the upper dumping layer is thick, and the rock soil is softly consolidated. This characteristic makes forming boreholes difficult and requires much ineffective drilling work, limiting the implementation of an exploration schedule. Moreover, the dumps along the roadside will be demolished in the next few years, therefore, this system does not allow for long-term observation. To the south of the roadside of the stope, due to the uplift of the strata and the partial development of the 5th coal seam group and the upper conglomerate section, the key area of this exploration is consistent with the direction of mining. Parameters such as the coordinates and the length of drilling are shown in Table 7.

In areas where the water quality is not good and water resources are limited, people should pay close attention to avoid penetrating the coal seam aquifer when digging wells to obtain reliable water. If necessary, measures may be needed to grout and seal the coal seam wall to prevent unqualified water from penetrating into the well. From a mining perspective, improvements and adjustments to the production process are required to reduce the amount of mine drainage, and water-saving measures should be taken within the mining area. The sewage from the mine must be processed to a level to be suitable for irrigation. Herdsmen should raise awareness of water conservation, adopt water-saving measures and tools advocated by the government, and make reasonable decisions about the basic area that can be reached by a well and control their amount of livestock based on the type of pasture and the type of livestock.

5. Conclusions

The groundwater quality of the North Power Shengli coal mine district was examined to assess its suitability for drinking and irrigation purposes. The results of the chemical analysis of groundwater samples revealed that the majority of the samples belonged to the $\text{Ca}^{2+}\text{-Mg}^{2+}\text{-HCO}_3^-$

Table 7
Parameter list of drilling coordinates and length

Hole label	X	Y	Z	H	Aquifer
KS1	420105	4871978	992	20	Quaternary pore aquifer
KS2	419810	4872439	1005	40	Top conglomerate segment aquifer
KS3	419328	4872716	1011	20	Quaternary pore aquifer
KS4	418873	4872413	1018	20	
KS5	418572	4873398	1023	15	No. 5 seam fracture confined aquifer
KS6	416991	4872334	1061	108	
KS7	416814	4872214	1070	150	
KS8	418673	4873705	1024	20	Quaternary pore aquifer
KS9	418210	4873399	1032	30	
KS10	416870	4872499	1032	40	
KS11	418132	4874070	1044	70	Top conglomerate segment aquifer
KS12	417441	4873604	1045	70	
KS13	416598	4873037	1068	100	
KS14	416500	4872970	1070	110	
KS15	417806	4874561	1045	140	No. 5 seam fracture confined aquifer
KS16	417435	4874558	1050	140	
KS17	416839	4874555	1078	200	
KS18	415994	4874547	1120	240	
KS19	419894	4876605	1060	250	Top conglomerate segment aquifer
KS20	420854	4876616	991	20	Quaternary pore aquifer
KS21	421058	4877740	982	25	
KS22	422575	4877061	976	100	No. 6 seam fracture confined aquifer
KS23	421698	4873883	982	97	No. 5 seam fracture confined aquifer
KSG1	417466	4873620	1045	50	Top conglomerate segment aquifer
KSG2	416864	4874570	1080	50	No. 5 seam fracture confined aquifer
KSG3	419129	4877852	1025	40	Top conglomerate segment aquifer

and $\text{Na}^+\text{-Cl}^-$ hydro-chemical facies. The surface water and groundwater have high concentrations of Na^+ , HCO_3^- and SO_4^{2-} , which almost exceed the maximum values of the WHO and GB 5749-2006 standards.

The distributions of major anions and cations and their ratios indicate that the groundwater in this region is more

strongly affected by carbonate sources. The distribution of $\gamma\text{SO}_4^{2-}/\gamma\text{Cl}^-$ also indicates that there are sulfate-producing minerals in the deep part of the strata. Chemical correlation analysis shows that local high Na^+ concentrations may be caused by the weathering and dissolution of rock minerals and the ion exchange of Ca^{2+} and Mg^{2+} in the soil. Local climatic conditions are also an important reason for the high background value of groundwater.

The detection of major ions (e.g., Ca^{2+} , Na^+ and SO_4^{2-}) and the calculation of water quality parameters (SAR, EC and % Na^+) indicate that the water from the shallow aquifer and surface water in this area are characterized by high salinity, low and medium alkalinity, and low conductivity and can thus be used for irrigation. However, the deep groundwater in this region (Permissible to Doubtful) has high salinity and alkalinity, and it is suitable for irrigation only after undergoing appropriate processing. The water from the coal seam aquifer is not suitable for irrigation due to its high salinity, high alkalinity and high conductance, but this does not mean that coal mining will result in groundwater being unsuitable for irrigation. In contrast, for the large coal bases in the steppe area, water drainage in the mining area is an important alternative to alleviate water use pressure. To establish and improve the groundwater monitoring network in the mining area and even around surrounding cities, the post-treatment of the coal seam aquifer drainage should be fully considered. When herdsman dig wells to fetch water, the drilling depth should be higher than the buried depth of the coal seam aquifer. Otherwise, the drilling method of blocking the pore wall of the coal seam aquifer should be adopted to fully avoid the water source of the coal seam aquifer and ensure the safety of living and irrigation water.

Acknowledgements

Our deepest gratitude goes to the editors and the anonymous reviewers for their careful work and thoughtful suggestions that have helped improve this paper substantially. The authors also gratefully acknowledge the financial support of National Key Research and Development Program (Grant No.2016YFC0501102), National Science and Technology Major Project (Grant No.2016ZX05066-001), Coal United Project of National Natural Science Foundation (Grant No.U1261203), Shanxi Natural Science Funds Project (Grant No. 2013012001).

References

- [1] S. Siebert, J. Burke, J.M. Faures, K. Frenken, J. Hoogeveen, P. Döll, F.T. Portmann, Groundwater use for irrigation - a global inventory, *Hydrol. Earth. Syst. Sci. Discuss.*, 7 (2010) 3977–4021.
- [2] J. Wang, L.I. Baolin, Y.U. Wanli, Analysis of vegetation trend and their causes during recent 30 years in inner mongolia autonomous region, *J. Arid. Land Resour. Environ.*, 26 (2012) 132–138.
- [3] Z. Fan, Z. Yang, X. Liu, L.I. Shihai, Z. Xin, Analysis of landslide mechanisms of the southern red bed slope in the No. 2 open-cast coal mine in eastern Shengli coal field, *Chin. J. Rock Mech. Eng.*, 35 (2016) 4063–4072.
- [4] Y.U. Peng, G. Shi, X.U. Jinjun, J. Tang, Study on water control and comprehensive treatment in shengli open-pit coal mine, *Opencast Min. Technol.*, 32 (2017) 67–70.
- [5] D. Kofke, E. Glandt, Monte carlo simulation of multicomponent equilibria in a semigrand canonical ensemble, *Mol. Phys.*, 64 (1988) 1105–1131.
- [6] T.J. Wolery, EQ3NR, a computer program for geochemical aqueous speciation-solubility calculations: Theoretical manual, user's guide, and related documentation (Version 7.0), Part 3, Lawrence Livermore National Laboratory, California, 1992.
- [7] M.A.H. Bhuiyan, M.A. Islam, S.B. Dampare, L. Parvez, S. Suzuki, Evaluation of hazardous metal pollution in irrigation and drinking water systems in the vicinity of a coal mine area of northwestern Bangladesh, *J. Hazard. Mater.*, 179 (2010) 1065–1077.
- [8] T. Marković, Ž. Brkić, O. Larva, Using hydro-chemical data and modelling to enhance the knowledge of groundwater flow and quality in an alluvial aquifer of zagreb, Croatia, *Sci. Total Environ.*, 458–460 (2013) 508–516.
- [9] E.S. Shanyengana, M.K. Seely, R.D. Sanderson, Major-ion chemistry and ground-water salinization in ephemeral floodplains in some arid regions of namibia, *J. Arid Environ.*, 57 (2004) 211–223.
- [10] J.L. Vanderzalm, B.M. Jeuken, J.D.H. Wischusen, P. Pavelic, C.L.G.L. Salle, A. Knapton, P.J. Dillon, Recharge sources and hydrogeochemical evolution of groundwater in alluvial basins in arid central Australia, *J. Hydrol.*, 397 (2011) 71–82.
- [11] V. Cloutier, R. Lefebvre, R. Therrien, M.M. Savard, Multivariate statistical analysis of geochemical data as indicative of the hydrogeochemical evolution of groundwater in a sedimentary rock aquifer system, *J. Hydrol.*, 353 (2008) 294–313.
- [12] O. Neves, M.J. Matias, Assessment of groundwater quality and contamination problems ascribed to an abandoned uranium mine (Cunha Baixa region, Central Portugal), *Environ. Geol.*, 53 (2008) 1799–1810.
- [13] A.K. Singh, B. Neogi, G.C. Mondal, T.B. Singh, Hydrogeochemistry, Elemental flux, and quality assessment of mine water in the pootkee-balihari mining area, Jharia Coalfield, India, *Mine. Water Environ.*, 30 (2011) 197–207.
- [14] V.B. Singh, A.L. Ramanathan, P. Sharma, Major ion chemistry and assessment of weathering processes of the patsio glacier melt water, Western Himalaya, India, *Environ. Earth. Sci.*, 73 (2015) 1–11.
- [15] B. Neogi, A.K. Singh, D.D. Pathak, A. Chaturvedi, Hydrogeochemistry of coal mine water of North karanpura coalfields, India: implication for solute acquisition processes, dissolved fluxes and water quality assessment, *Environ. Earth. Sci.*, 76 (2017) 489.
- [16] A.K. Tiwari, M.D. Maio, P.K. Singh, A.K. Singh, Hydrogeochemical characterization and groundwater quality assessment in a coal mining area, India, *Arab. J. Geosci.*, 9 (2016) 1–17.
- [17] S. Jiang, X. Kong, H. Ye, N. Zhou, Groundwater dewatering optimization in the Shengli no. 1 open-pit, coalmine, Inner Mongolia, China, *Environ. Earth. Sci.*, 69 (2013) 187–196.
- [18] H. Qi, R. Hu, Q. Zhang, Concentration and distribution of trace elements in lignite from the shengli coalfield, Inner Mongolia, China: Implications on origin of the associated Wulantuga Germanium Deposit, *Int. J. Coal Geol.*, 71 (2007) 129–152.
- [19] H. Qi, R. Hu, Q. Zhang, REE geochemistry of the cretaceous lignite from wulantuga germanium deposit, inner mongolia, Northeastern China, *Int. J. Coal Geol.*, 71 (2007) 329–344.
- [20] Z. Yang, S.W. Niu, H.L. Chang, Z.G. Liu, Evaluation of sustainability of the regional ecological economics development based on the ecological footprint model, *Econ. Geogr.*, 25 (2005) 542–547.
- [21] H.G. Gorchev, G. Ozolins, WHO guidelines for drinking-water quality, *WHO Chron.*, 38 (1984) 104–108.
- [22] B. Zhang, X. Song, Y. Zhang, D. Han, C. Tang, Y. Yu, Y. Ma, Hydro-chemical characteristics and water quality assessment of surface water and groundwater in Songnen plain, Northeast China, *Water Res.*, 46 (2012) 2737–2748.
- [23] B.J. Graupner, C. Koch, H. Prommer, Prediction of diffuse sulfate emissions from a former mining district and associated groundwater discharges to surface waters, *J. Hydrol.*, 513 (2014) 169–178.

- [24] S.T. Kivi, R.T. Bailey, Modeling sulfur cycling and sulfate reactive transport in an agricultural groundwater system, *Agric. Water Manag.*, 185 (2017) 78–92.
- [25] J.A. Morales, L.S. de Graterol, J. Mesa, Determination of chloride, sulfate and nitrate in groundwater samples by ion chromatography, *J. Chromatogr. A.*, 884 (2000) 185–190.
- [26] Y. Wang, M.A. Shao, Z. Liu, D.N. Warrington, Investigation of factors controlling the regional-scale distribution of dried soil layers under forestland on the loess plateau, China, *Surv. Geophys.*, 33 (2012) 311–330.
- [27] H.C. Emvoutou, B.K. Tandia, S.N.B. Nkot, R.C.S. Ebonji, Y.B. Nlend, G.E. Ekodeck, C. Stumpp, P. Maloszewski, S. Faye, Geologic factors controlling groundwater chemistry in the coastal aquifer system of Douala/Cameroon: implication for groundwater system functioning, *Environ. Earth. Sci.*, 77 (2018) 219.
- [28] A. Peralta-Tapia, R.A. Sponseller, A. Ågren, D. Tetzlaff, C. Soulsby, H. Laudon, Scale-dependent groundwater contributions influence patterns of winter base flow stream chemistry in boreal catchments, *J. Geophys. Res.*, 120 (2015) 847–858.
- [29] P. Ravikumar, K. Venkatesharaju, R.K. Somashekar, Major ion chemistry and hydro-chemical studies of groundwater of Bangalore South Taluk, India, *Environ. Monit. Assess.*, 163 (2010) 643–653.
- [30] Y.S. Zheng, Temporal and spatial variation of groundwater depth in shiyang river basin, *Ground Water*, 39 (2017) 60–62.
- [31] L.J. Chen, Q. Feng, C.S. Li, Y.X. Song, W. Liu, J.H. Si, B.G. Zhang, Spatial variations of soil microbial activities in saline groundwater-irrigated soil ecosystem, *Environ. Manag.*, 57 (2016) 1–8.
- [32] G.X. Zhang, D. Wei, H.E. Yan, R. Salama, Hydro-chemical characteristics and evolution laws of groundwater in songnen plain, Northeast China, *Adv. Water Sci.*, 17 (2006) 20–28.
- [33] H.M. Mahdi, N. Ahmad, Studying the effect of drought on water resources over two decades and occurrences of the sinking phenomenon in minab plain, *Environ. Sci.*, 9 (2012) 75–98.
- [34] H. Torkamanitombeki, J. Rahnamarad, N. Saadatkhah, Groundwater chemical indices changed due to water-level decline, Minab Plain, Iran, *Environ. Earth. Sci.*, 77 (2018) 269.
- [35] B.K. Rana, M.R. Dhumale, P. Lenka, S.K. Sahoo, P.M. Ravi, R.M. Tripathi, A study of natural uranium content in groundwater around Tummalapalle uranium mining and processing facility, India, *J. Radioanal. Nucl. Ch.*, 307 (2016) 1–8.
- [36] A.K. Singh, N.P. Varma, G.C. Mondal, Hydrogeochemical investigation and quality assessment of mine water resources in the Korba coalfield, India, *Arab. J. Geosci.*, 9 (2016) 1–20.
- [37] G.P. Williams, K. Petteys, C.H. Gammons, S.R. Parker, An investigation of acidic head-water streams in the Judith Mountains, Montana, USA, *Appl. Geochem.*, 62 (2015) 48–60.
- [38] C.M. Cheng, M. Amaya, T. Butalia, R. Baker, H.W. Walker, J. Massey-Norton, W. Wolfe, Short-term influence of coal mine reclamation using coal combustion residues on groundwater quality, *Sci. Total Environ.*, 571 (2016) 834–854.
- [39] R. Jahanshahi, M. Zare, Assessment of heavy metals pollution in groundwater of Golgohar iron ore mine area, Iran, *Environ. Earth. Sci.*, 74 (2015) 505–520.
- [40] M. Behzad, M. Shiva, R. Behrouz, Y. Behrouz, Assessment of metal contamination in groundwater and soils in the Ahangaran mining district, west of Iran, *Environ. Monit. Assess.*, 187 (2015) 727.
- [41] B. Li, H. Shi, J. Zhang, Z. Li, Hydro-chemical characteristics of groundwater before and after water-saving reform in Hetao irrigation district, Inner Mongolia, *Trans. Chin. Soc. Agric. Eng.*, 30 (2014) 99–110.
- [42] Z. Zhang, H. Guo, W. Zhao, S. Liu, Y. Cao, Y. Jia, Influences of groundwater extraction on flow dynamics and arsenic levels in the western Hetao Basin, Inner Mongolia, China, *Hydrol. J.*, 26 (2018) 1–14.
- [43] A.M. Piper, A graphic procedure in the geochemical interpretation of water-analyses, *Neurochem. Int.*, 6 (1984) 27–39.
- [44] G. Sappa, S. Ergul, F. Ferranti, Water quality assessment of carbonate aquifers in southern Latium region, Central Italy: a case study for irrigation and drinking purposes, *Appl. Water. Sci.*, 4 (2014) 115–128.
- [45] Donovan, Todd, *The elements of social scientific thinking*, ST. MARTIN'S PR, London, 2004.
- [46] V. Bhuriya, P. Dev, Groundwater quality evaluation for agriculture/irrigation of meghnagar area, Jhabua Region, Madhya Pradesh, India, *Asian J. Multidiscip. Stud.*, 2 (2014) 35–41.
- [47] L. Wilcox, *Effect of industrial wastes on water for irrigation Use*, American Society for Testing Materials, Philadelphia PA, 1960.
- [48] W.T. McGeorge, Diagnosis and improvement of saline and alkaline soils, *Soil Sci. Soc. Am. J.*, 18 (1954) 348.